Rotor Position Feedback Over an RF Link for Motor Speed Control

Sudip K. Mazumder, *Senior Member, IEEE*, Rongjun Huang, *Student Member, IEEE*,
and Kaustuva Acharya

***Abstract*—In this paper, we demonstrate the feasibility of controlling the speed of an induction motor using a wireless position feedback over an RF link, and compare its performance under dynamic- and steady-state conditions with those obtained by using a wire-based position feedback control. The wireless scheme precludes the need for the cable that feeds the position from the sensor to the controller, thereby minimizing feedback noise pickup and cost for some applications. It also raises the possibility of using a low-resolution, low-cost sensor, which, along with the use of simple estimation algorithms, may potentially provide an alternative to or backup support for conventional position sensorless control for a wide range of motors and speeds. Further, using a composite Lyapunov-function-based approach, we determine the effect of time delay (due to wireless communication) on the stability of the overall system.**

***Index Terms*—Composite Lyapunov function, induction motor, linear matrix inequality, piecewise nonlinear system, position feedback, speed control, wireless network control.**

I. INTRODUCTION

SPEED control of an induction motor usually requires position feedback information [as illustrated in Fig. 1(a)] from an encoder, a resolver, or a Hall sensor to a controller unit [1]. These feedback signals, which often pickup noise due to electromagnetic interference, can affect the performance of the motor control system. As such, the feedback cable is shielded and the signals are provided in differential form, which increases the sensing cost. Therefore, motor-drive manufacturers have been focusing on position sensorless control [2], [3] [as illustrated in Fig. 1(b)]. However, *universal applicability* of the position sensorless algorithms for speed control, especially at or near-zero speed and at full-load torque, has not been fully achieved yet.

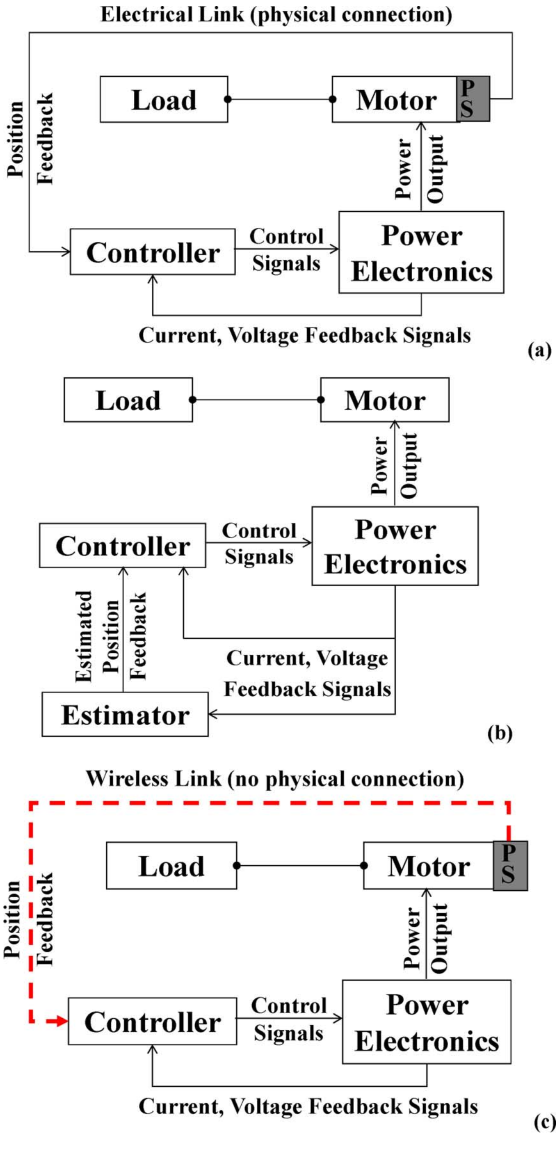

Fig. 1. Illustration of motor-control system (with internal control reference) with: (a) wire-based position feedback, (b) position estimation, and (c) wireless position feedback. PS stands for position sensor.

In this paper, we outline a technique [as illustrated in Fig. 1(c)] for implementing a Volts/Hertz (V/F) (i.e., constant flux) induction motor control [1], [4] using real-time wireless feedback of rotor position over an RF transmission link. Today, several

---

Manuscript received January 1, 2008. Current version published April 9, 2010. This work was supported by the Maintenance Requirement Cards–Caterpillar under Award 558953, and in part by the National Science Foundation CAREER Award under Award 0239131 and by the Office of Naval Research Young Investigator Award under Award N000140510594 received in the years 2002, 2003, and 2005, respectively. Recommended for publication by Associate Editor B. Tamyurek.

S. K. Mazumder is with the Laboratory for Energy and Switching-Electronics Systems, Department of Electrical and Computer Engineering, University of Illinois, Chicago, IL 60607 USA (e-mail: mazumder@ece.uic.edu).

R. Huang was with the Laboratory for Energy and Switching-Electronics Systems, Department of Electrical and Computer Engineering, University of Illinois, Chicago, IL 60607 USA. He is now with International Rectifier Corporation, El Segundo, CA 90245 USA (e-mail: rhuang1@irf.com).

K. Acharya was with the Laboratory for Energy and Switching-Electronics Systems, Department of Electrical and Computer Engineering, University of Illinois, Chicago, IL 60607 USA. He is now with Texas Instruments, Dallas, TX 75251 USA (e-mail: kachar1@uic.edu).

Color versions of one or more of the figures in this paper are available online at http://ieeexplore.ieee.org.

Digital Object Identifier 10.1109/TPEL.2009.2036178

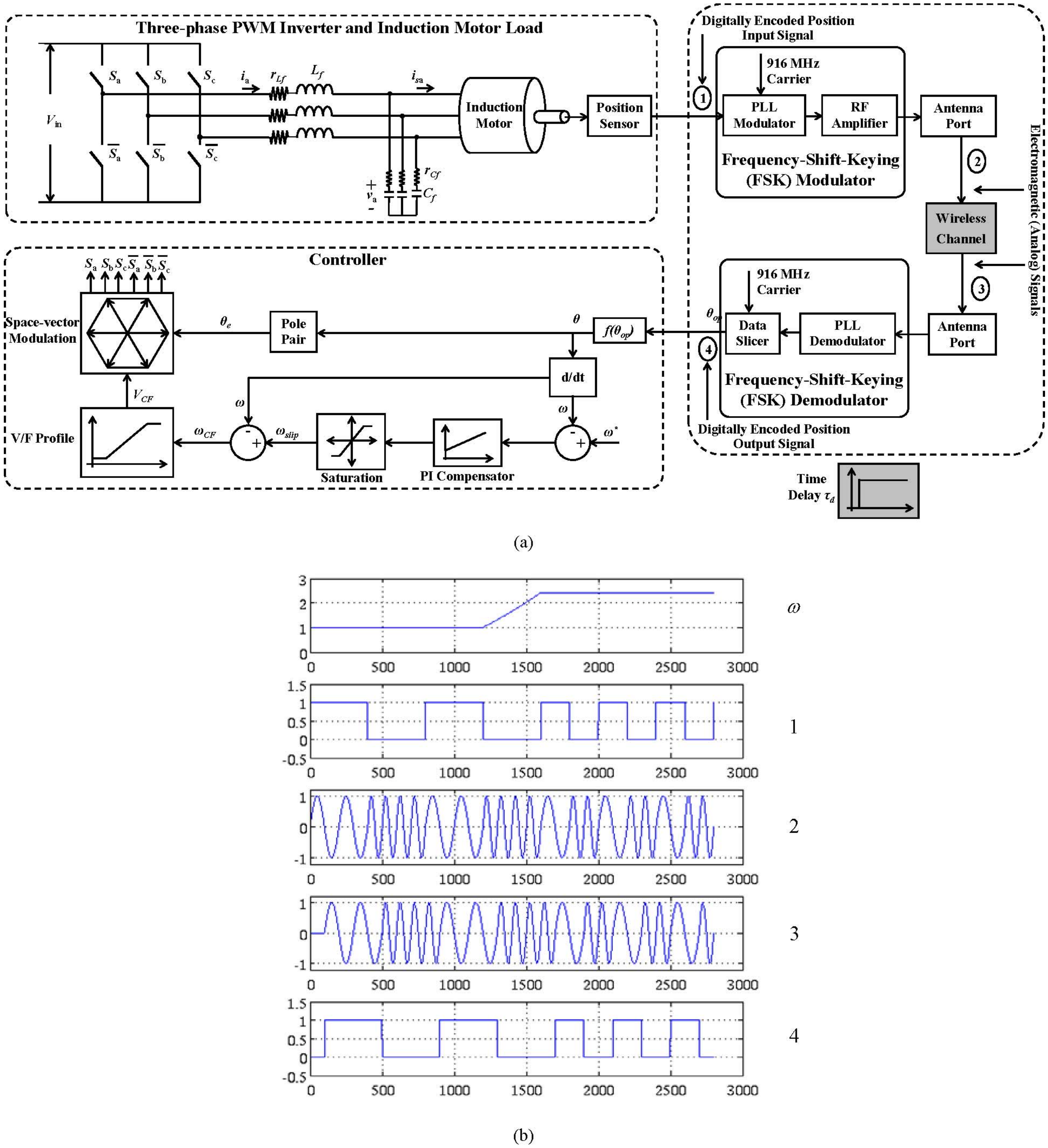

(a)

(b)

Fig. 2. (a) Block diagram of the overall system. (b) Wireless transmission scheme for position feedback along with key waveforms at points marked “1”–“4” and illustration of the end-to-end time delay (τ_d).

commercial and defense applications have addressed health monitoring and RF identification (RFID) of motors using a wireless link [5]–[7]. The proposed scheme can use the same RF channel (via hopping) to transmit the position feedback (typically over a 300-ft transmission range). This eliminates the need for a multiwire cable, which can be expensive, especially for harsh and extended operating conditions, and much costlier than a miniaturized RF transmitter. The proposed wireless position-sensing scheme can also be extended to other vector control schemes for induction and other motors.

Conventional position sensorless control schemes require complex estimation algorithms, and have limitations regarding the speed range and applicability. However, such schemes save the cost of an expensive position sensor. So, if a *low-cost, low-resolution position sensor* is used that transmits information over an RF link (thereby precluding the cable cost), then a simple position-estimation algorithm [2] operating along with the lower resolution but discrete-time-interval position updates can be potentially as powerful as the complex position sensorless control (which has no position feedback). Because the cost of the high-resolution sensor is higher to begin with, the proposed wireless information-exchange-based scheme, which can potentially use cheaper low-resolution sensors, can be a more cost-effective approach. However, because wireless transmission over an RF link is susceptible to channel disruptions [8], [9], it is important to investigate the impact of time delay on the stability and performance of the overall system, so that controllers can be designed to ensure operation within the desired bounds.

II. SYSTEM DESCRIPTION

Fig. 2(a) illustrates a schematic of the overall system consisting of an induction motor, a pulsewidth-modulated inverter, and a V/F feedback controller [4] that receives the motor position feedback over a wireless channel. We use frequency-shift-keying (FSK) [10] for RF transmission. As shown in Fig. 2(b), the square-wave output of the position encoder is first multiplexed and then fed to an RF transmitter. The RF receiver antenna is tuned to a transmission frequency of 900 MHz. The receiver demodulates and amplifies the broadcast signal, such that the output of the receiver matches the pattern of the original encoded digital signal. Finally, the demodulated signal is fed to the motor controller. In the absence of channel disruptions, the *(position-sensor-to-controller or end-to-end) time delay* (τ_d) is negligible, but it increases with deteriorating channel conditions or for reduced data rates. The RF receiver of the controller demodulates the received signal to extract the digitally encoded position feedback ($\theta_{\rm op}$). It is then transformed to a continuous domain using $\theta = f(\theta_{\rm op}) = \theta(0) + \text{MODULO}(\theta_{\rm op}, N_{\rm enc})(1/N_{\rm enc})360°$, where $N_{\rm enc}$ (=1024 for our case) represents the angular resolution of the encoder. The position feedback (θ) is fed to the controller that derives the velocity using $\omega = d\theta/dt$, which is then compared with the velocity reference (ω^*). The error between ω^* and ω is fed to a proportional–integral (PI) controller to obtain the slip, which is then added to ω to obtain the drive frequency ($\omega_{\rm CF}$). Subsequently, using $\omega_{\rm CF}$, a desired voltage-reference magnitude ($V_{\rm CF}$) is generated to maintain a V/F operation [1] of the induction motor. Voltage reference $V_{\rm CF}$ and its instantaneous electrical position (i.e., $\theta_e = p\theta/2$, where p represents the number of motor poles) are fed to a space-vector modulation (SVM) block to obtain the switching signals of the inverter.

III. TIME DELAY STABILITY BOUND USING A PIECEWISE NONLINEAR MODEL

To apply the composite Lyapunov-function-based methodology (outlined later) for ascertaining the impact of end-to-end time delay on the stability of the overall system (comprising the induction motor [11], the three-phase inverter [12], and the linear compensator for V/F control), we represent (following [13]) the system model in a dq (synchronous frame) frame as a weighted sum of piecewise linear models:

$$\dot{e} = \sum_{j=0}^{r} w_j(e)\left(A_{0jl}e + A_{1jl}e\left(t - \tau_d\right) + B_{jl}\right) \tag{1}$$

TABLE I
DEFINITION OF THE SYMBOLS FOR THE MOTOR MODEL

State Description	***State***	***Reference***	***State in Error coordinates***
Inverter output current (*d*-axis)	i_d	i_d^*	$e_{i_d} = i_d^* - i_d$
Inverter output current (*q*-axis)	i_q	i_q^*	$e_{i_q} = i_q^* - i_q$
Inverter output voltage (*d*-axis)	v_d	v_d^*	$e_{v_d} = v_d^* - v_d$
Inverter output voltage (*q*-axis)	v_q	v_q^*	$e_{v_q} = v_q^* - v_q$
Stator current (*d*-axis)	i_{sd}	i_{sd}^*	$e_{i_{sd}} = i_{sd}^* - i_{sd}$
Stator current (*q*-axis)	i_{sq}	i_{sq}^*	$e_{i_{sq}} = i_{sq}^* - i_{sq}$
Rotor current (*d*-axis)	i_{rd}	i_{rd}^*	$e_{i_{rd}} = i_{rd}^* - i_{rd}$
Rotor current (*q*-axis)	i_{rq}	i_{rq}^*	$e_{i_{rq}} = i_{rq}^* - i_{rq}$
Rotor speed	ω	ω^*	$e_\omega = \omega^* - \omega$
Controller state	ξ_1	ξ_1^*	$e_{\xi_1} = \xi_1^* - \xi_1$

where $r = 4$, l represents the switching states of the inverter and $e = [e_{i_d}\ e_{i_q}\ e_{v_d}\ e_{v_q}\ e_{i_{sd}}\ e_{i_{sq}}\ e_{i_{rd}}\ e_{i_{rq}}\ e_\omega\ e_{\xi_1}]^T$. The states of the overall system are defined in Table I. Functions $w_0(e) = 1$, $w_1(e) = (\omega^* - e_\omega)$, $w_2(e) = (\omega^* - e_\omega)^{-1}$, $w_3(e) = (i_{\rm rd}^* - i_{\rm rd})$, and $w_4(e) = (i_{\rm sd}^* - i_{\rm sd})$, while the matrices $A_{0jl}(e)$, A_{1jl}, and B_{jl} are defined in Table II.

Next, using (1), we investigate the stability of the overall system using a composite Lyapunov-function-based approach [14]. For the *j*th subsystem, we define a composite Lyapunov function $V_{kj}(e) > 0$, i.e.,

$$V_{kj}(e) = \sum_{l=1}^{h} \alpha_{kjl} e^T P_{kjl} e \Bigg(k = 1, 2, \ldots, M; \sum_{l=1}^{h} \alpha_{kjl} = 1; \text{ and } 0 \le \alpha_{kjl} \le 1 \Bigg) \tag{2}$$

where P_{kjl} is a positive-definite matrix, *k* represents a particular switching sequence, and h represents the number of switching states in a given switching sequence. The overall system described by (1) is stable provided $\dot{V}_{kj}(e) < 0$, which is ensured provided the following matrix inequality is satisfied [14] for any $\gamma > 0, p > 1$:

$$\sum_{l=1}^{h} \alpha_{kjl} \times \begin{bmatrix} G_{kjl} & P_{kjl}A_{1jl}A_{0jl} & -P_{kjl}A_{1jl}^2 & P_{kjl}B_{jl} \\ -A_{0jl}^T A_{1jl}^T P_{kjl} & -\gamma p P_{kjl} & 0 & 0 \\ -\left(A_{1jl}^2\right)^T P_{kjl} & 0 & -\gamma P_{kjl} & 0 \\ \bar{B}_{jl}^T P_{kj} & 0 & 0 & 0 \end{bmatrix} < 0 \tag{3}$$

where $G_{kjl} = \frac{1}{\tau_d}[(A_{0jl} + A_{1jl})^T P_{kjl} + P_{kjl}(A_{0jl} + A_{1jl})] +$

TABLE II
DEFINITION OF THE MATRICES IN (1)

$A_{00l}(e)=\begin{bmatrix} -\frac{r_{Lf}}{L_f} & 0 & -\frac{1}{L_f} & 0 & 0 & 0 & 0 & 0 & 0 & 0 \\ 0 & -\frac{r_{Lf}}{L_f} & 0 & -\frac{1}{L_f} & 0 & 0 & 0 & 0 & 0 & 0 \\ \frac{1}{C_f} & 0 & 0 & 0 & -\frac{1}{C_f} & 0 & 0 & 0 & 0 & 0 \\ 0 & \frac{1}{C_f} & 0 & 0 & 0 & -\frac{1}{C_f} & 0 & 0 & 0 & 0 \\ 0 & 0 & -a_1 & 0 & 0 & \frac{a_1}{R_s} & 0 & \frac{-a_3}{R_r} & 0 & 0 \\ 0 & 0 & 0 & -a_1 & \frac{a_1}{R_s} & 0 & \frac{-a_3}{R_r} & 0 & 0 & 0 \\ 0 & 0 & a_3 & 0 & 0 & \frac{-a_3}{R_s} & 0 & \frac{a_4}{R_r} & 0 & 0 \\ 0 & 0 & 0 & a_3 & \frac{-a_3}{R_s} & 0 & \frac{a_4}{R_r} & 0 & 0 & 0 \\ 0 & 0 & 0 & 0 & 0 & 0 & 0 & 0 & 0 & 0 \\ 0 & 0 & 0 & 0 & 0 & 0 & 0 & 0 & \varepsilon & -K_i \end{bmatrix}$ where $a_1=\frac{L_r}{\left(L_m^2-L_sL_r\right)},\ a_2=\frac{L_m^2}{\left(L_m^2-L_sL_r\right)},\ a_3=\frac{L_m}{\left(L_m^2-L_sL_r\right)},\ a_4=\frac{L_s}{\left(L_m^2-L_sL_r\right)}$	$A_{01l}(e)=\begin{bmatrix} \begin{matrix} 0 & 1 & 0 & 0 \\ -1 & 0 & 0 & 0 \\ 0 & 0 & 0 & 1 \\ 0 & 0 & -1 & 0 \end{matrix} & 0_{4\times6} \\ 0_{6\times4} & 0_{6\times6} \end{bmatrix}$ $A_{02l}(e)=\begin{bmatrix} 0_{4\times4} & 0_{4\times4} & 0_{4\times2} \\ 0_{4\times4} & \begin{matrix} -a_2 & 0 & \frac{-a_3}{L_r} & 0 \\ 0 & a_2 & 0 & \frac{a_3}{L_r} \\ \frac{a_4}{L_m} & 0 & \frac{a_4}{L_r} & 0 \\ 0 & \frac{-a_4}{L_m} & 0 & \frac{-a_4}{L_r} \end{matrix} & 0_{4\times2} \\ 0_{2\times4} & 0_{2\times4} & 0_{2\times2} \end{bmatrix}$ $A_{03l}(e)=\begin{bmatrix} 0_{8\times5} & 0_{8\times5} \\ 0_{2\times5} & \begin{matrix} \frac{3}{2J}\left(\frac{p}{2}\right)L_m & 0 & 0 & 0 & 0 \\ 0 & 0 & 0 & 0 & 0 \end{matrix} \end{bmatrix}$ $A_{04l}(e)=\begin{bmatrix} 0_{8\times5} & 0_{8\times5} \\ 0_{2\times5} & \begin{matrix} 0 & 0 & \frac{3}{2J}\left(\frac{p}{2}\right)L_m & 0 & 0 \\ 0 & 0 & 0 & 0 & 0 \end{matrix} \end{bmatrix}$
$A_{10l}=A_{11l}=A_{12l}=A_{13l}=A_{14l}=\begin{bmatrix} 0_{10\times8} & \begin{matrix} 0_{2\times9} \\ -1 \quad 0 \end{matrix} \end{bmatrix}$	
$B_{0l}=-\begin{bmatrix} \frac{4}{3L_1}\left(S_d-\frac{1}{2}S_q\right)V_{in} & \frac{4}{3L_1}\left(S_q-\frac{1}{2}S_d\right)V_{in} & 0_{1\times7} & \omega^* \end{bmatrix}^T-\left(A_{00l}+A_{10l}\right)x^*$	
$B_{1l}=-A_{01l}x^*,\ B_{2l}=-A_{02l}x^*,\ B_{3l}=-A_{03l}x^*,\ B_{4l}=-A_{04l}x^*.$	

Symbol definitions are as follows: x^* represent the reference values of the states outlined in Table I; S_d and S_q are the switching functions of the inverter in the synchronous reference frame, respectively; L_f and C_f are the filter inductance and capacitance, respectively; r_{Lf} and r_{Cf} are the parasitic resistances of L_f and C_f respectively; R_s and R_r are stator and rotor resistances, respectively; L_s, L_r, and L_m are the stator, rotor, and magnetizing inductances, respectively; V_{in} is the bus voltage; J represents the combined moment of inertia; and ω is the motor speed.

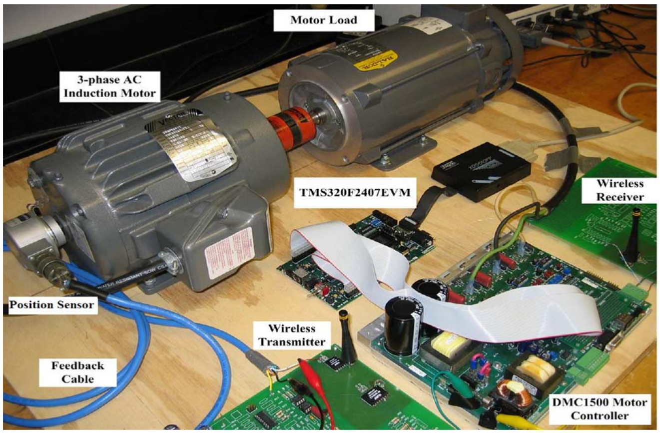

Fig. 3. Experimental setup.

$(\gamma p+\gamma)P_{kjl}$. By varying τ_d in (3), we determine the stable and unstable regions of operation of the overall system.

IV. RESULTS

Fig. 3 shows the experimental setup consisting of the induction motor fed by a DMC1500 inverter (developed by Spectrum Digital, Inc.) with a dc motor that serves as the load. The control inputs to this inverter are provided by the TMS320LF2407EVM DSP board (also available from Spectrum Digital, Inc.), which implements the V/F speed controller that is outlined in Section II. The induction motor parameters are as follows: three-phase, 230 V, 4-pole ($p=4$), 60 Hz, 1 HP, $R_r=9.91\ \Omega$, $R_s=6.62\ \Omega$, $L_s=24.2764$ mH, $L_r=19.5787$ mH, $L_m=750.62778$ mH, and $J=0.142$ kg·m^2. The parameters for the three-phase inverter and line filter are as follows: $V_{\text{in}}=400$ V, f_s (switching frequency) $=10$ kHz, $L_f=1.5$ mH, $C_f=0.1\ \mu$H, $r_{\text{Lf}}=10$ mΩ, and $r_{\text{Cf}}=0.5$ mΩ. For wireless position sensing, a low-cost LINX TXM-916-ES transceiver is used with a baud rate of 56 Kb/s and transmission frequency of 916 MHz.

To evaluate the efficacy of the wireless position feedback scheme, we compare its performance with a wire-based scheme. Fig. 4 illustrates that the percentage error in speed, expressed as $\frac{1}{T_w}\sqrt{\int_0^{T_w}\left(\frac{e_\omega}{\omega^*}\right)^2dt}\times 100$ (where $e_\omega=\omega^*-\omega$ and T_w represents the time window for calculation), versus the motor speed (ω) using wire-based and wireless position-sensing schemes (with channel separations of 0.2 and ≈7 ft for the later) are consistent.

We note that the digital word corresponding to $\omega=d\theta/dt$ (in the DSP controller) is obtained by following the industrial practice of taking the difference between two successive samples of θ, since the sampling interval is fixed using a timer.

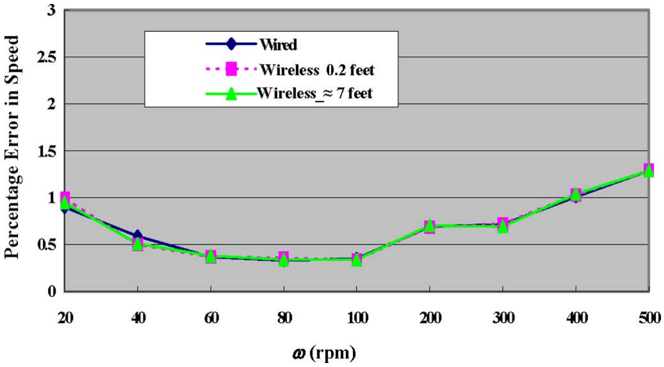

Fig. 4. Percentage error in speed versus ω for wire-based and wireless feedback control systems. For the latter, the measurements are obtained for channel separations of 0.2 and ≈7 ft, and the measured value of τ_d is found to be less than 100 μs. The delay is measured by plotting the transmitted and received position signals on the same oscilloscope, as illustrated in Fig. 2.

The consistency in the performance of the wire-based and wireless position-sensing schemes can be explained by observing that the experimental averaged SVM output (top) and motor-phase-current (bottom) waveforms shown in Fig. 5(a) and (b) are similar. For this result, the motor speed is set at 500 r/min, while $\tau_d < 100$ μs. Interestingly, and as shown in Fig. 5(c), the noise content of the position feedback signals (pulses) in the case of the wire-based position feedback is higher than that obtained using the wireless position sensing.

Next, we evaluate the transient performance of the wire-based and wireless position-sensing schemes. Fig. 6 illustrates the transient response when the motor speed changes from 300 to 500 r/min and back to 200 r/min. Fig. 6 illustrates that the dynamic performance of the motor for both mechanisms of position sensing are close, thus illustrating the feasibility of the wireless-position-feedback-based speed control.

So far, we have considered cases where the communication network operates in its nominal operating condition, i.e., where the time delay (τ_d) is negligible. However, the communication channel can be subjected to disruptions, which can be artificial (for instance, due to channel jamming by a rogue node) or due to deteriorating environmental conditions. For such cases, the time delay due to the wireless communication channel could increase. Therefore, it is important to determine the impacts of time delay on the global stability and performance of the system. Fig. 7(a) illustrates the variation of the maximum stable value of time delay ($\tau_{d\,\max}$) with motor speed, which is obtained using the composite Lyapunov-function-based technique described in Section III. We observe that $\tau_{d\,\max}$ reduces with increasing motor speed, which has implications on the upper limit on operating speed for a given time delay. Next, using parametric simulations, we evaluate the performance of the system (operating within the stability boundary) for varying τ_d and ω, and compare it with a wire-based approach (which corresponds to $\tau_d = 0$). Fig. 7(b) shows the relation among the percentage error in speed, ω, and τ_d. We observe that, even for a large end-to-end time delay, the speed regulation over a wide range of motor speeds is fairly good and consistent.

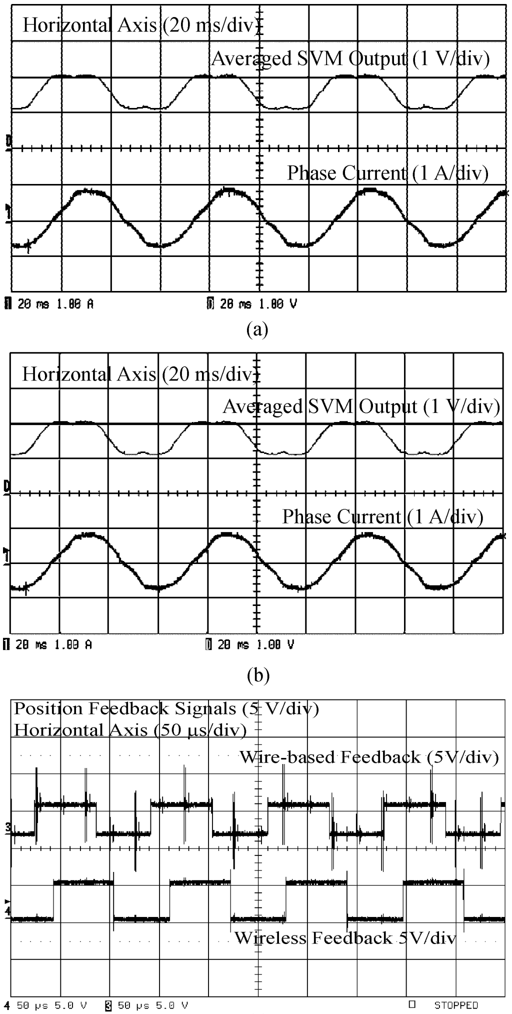

(a)

(b)

(c)

Fig. 5. Averaged SVM output and phase current of the induction motor using: (a) wireless and (b) wire-based position feedbacks. (c) Noise pickup in position-feedback signals for wire-based and wireless control schemes. The motor speed is regulated at 500 r/min.

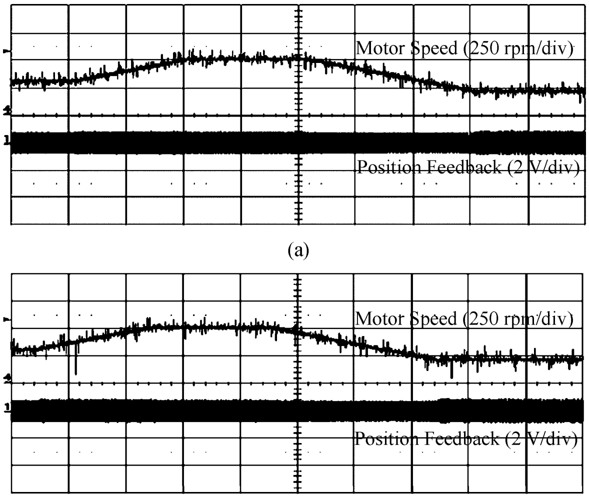

(a)

(b)

Fig. 6. Dynamic responses of the motor using: (a) wire-based and (b) wireless position-feedback control. Time delay (τ_d) in this case is measured to be less than 100 μs.

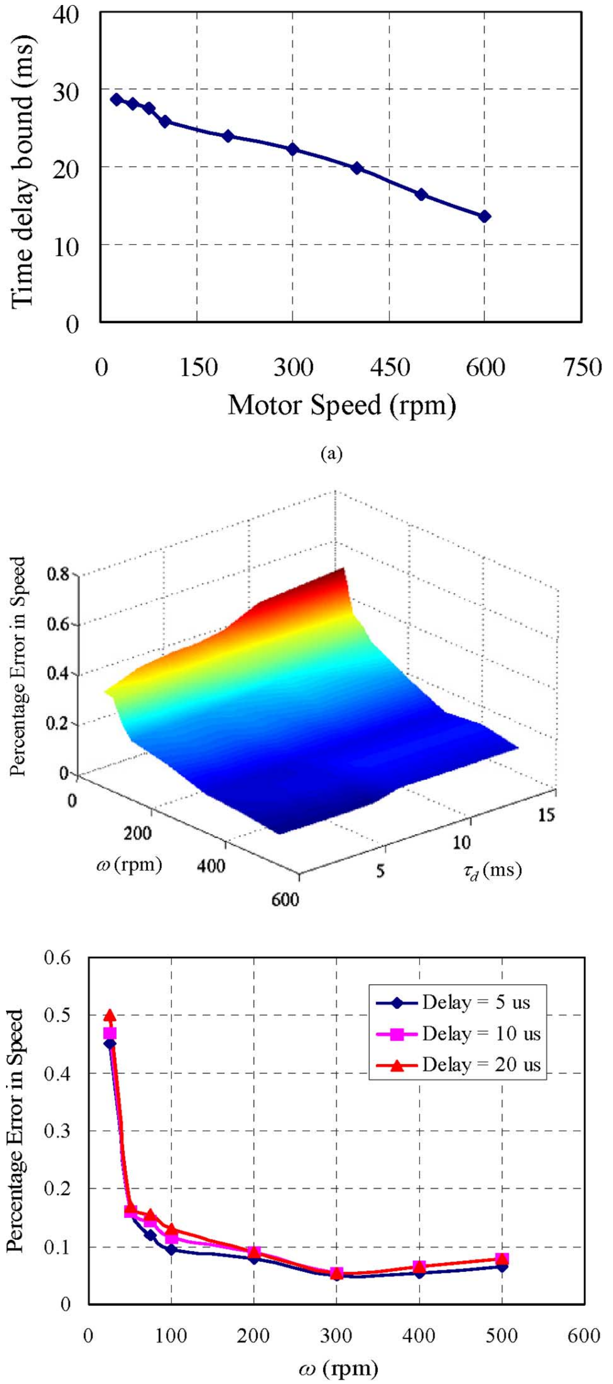

(a)

(b)

Fig. 7. (a) Stability boundary obtained by determining the maximum value of τ_d for a given speed at which the system is unstable. (b) Percentage error in speed versus the motor speed and end-to-end time delay (τ_d). Time delay $\tau_d = 0$ corresponds to the wire-based feedback control scheme, while the remaining time delays could occur in the wireless feedback control scheme, depending on the channel condition and data rate.

V. SUMMARY AND CONCLUSION

We demonstrate the feasibility of an induction motor speed control scheme using wireless position feedback, and compare its performance with those obtained by using a wire-based position feedback. Although the wireless sensing scheme precludes the need for a multiwire physical connection (thereby saving cost), the performance of the motor using this scheme is very close to that obtained by using wire-based position feedback. Although the wireless scheme is applicable up to zero speed, in this paper, the lower speed limit of 20 r/min (~0.3333 Hz) was used because of the lower bandwidth limitation of the analog RF transmitter. Our recent work in [15] with complete digital implementation overcomes this limitation.

Under good channel conditions and within the bandwidth of the RF transceiver, the noise pickup of the feedback position signal (within the RF transmission range) is found to be lower for the wireless-sensing scheme, which also exhibits little sensitivity to the channel separation between the transmitter and receiver units. Thus, although channel disruption in the wireless scheme causes data loss (and delay), successfully transmitted data pick up less noise than data transmitted using wire-based feedback. This is because in the wireless scheme, there is no involvement of cable for data transmission.

For the same channel conditions, RF transmission incurs a small *position-sensor-to-controller* time delay (τ_d), but it has no tangible effect on motor performance. However, when τ_d increases (e.g., due to deteriorating channel conditions or a reduced data rate), the time delay stability bound of the system reduces with increasing motor speed. This has implications on how slow the nominal data rate can be and the upper limit on operating speed for a given τ_d. However, our parametric simulations illustrating the functional relationship among speed regulation, motor speed, and τ_d show that the overall performance of the motor control system using wireless position sensing is reasonably good even under a significant time delay and over a wide range of operating speeds.

ACKNOWLEDGMENT

Any opinions, findings, conclusions, or recommendations expressed herein are those of the authors and do not necessarily reflect the views of Maintenance Requirement Cards–Caterpillar, National Science Foundation, and Office of Naval Research.

REFERENCES

[1] W. Leonhard, *Control of Electrical Drives*. New York: Springer-Verlag, 1996.

[2] P. Vas, *Sensorless Vector and Direct Torque Control*. London, U.K.: Oxford Univ. Press, 1998.

[3] K. Rajashekara, A. Kawamura, and K. Matsuse, *Sensorless Control of AC Motor Drives: Speed and Position Sensorless Operation*. Piscataway, NJ: IEEE Press, 1996.

[4] Digital control system group, “ACI3–1 system documentation—Variable speed control of 3-phase AC induction motor,” Texas Instrument, Villeneuve-Loubet Cedex, France, Project Rep., Sep. 2000.

[5] B. Lu, T. G. Habetler, R. G. Harley, and J. A. Gutirrez, “On the application of wireless sensors networks in condition monitoring and energy usage evaluation for electric machines,” in *Proc. IEEE Ind. Appl. Soc. Conf.*, 2005, pp. 2674–2679.

[6] B. Nickerson and R. Lally, “Development of a smart wireless networkable sensor for aircraft engine health management,” in *Proc. IEEE Aerosp. Conf.*, 2001, pp. 3255–3262.

[7] H. Ramamurthy, B. S. Prabhu, R. Gadh, and A. M. Madni, “Wireless industrial monitoring and control using a smart sensor platform,” *IEEE Sensors J.*, vol. 7, no. 5, pp. 611–618, May 2007.

[8] S. K. Mazumder, K. Acharya, and M. Tahir, "Wireless control of spatially distributed power electronics," in *Proc. IEEE Appl. Power Electron. Conf.*, 2005, pp. 75–81.

[9] K. Acharya, S. K. Mazumder, and M. Tahir, "Fault-tolerant wireless network control of load-sharing multiphase interactive power network," in *Proc. IEEE Power Electron. Spec. Conf.*, 2006, pp. 1167–1174.

[10] T. S. Rappaport, *Wireless Communications—Principles and Practice*, 2nd ed. Englewood Cliffs, NJ: Prentice-Hall, 2001.

[11] P. Pillay and V. Levin, "Mathematical models for induction machines," in *Proc. IEEE Ind. Appl. Soc. Conf.*, 1995, pp. 606–616.

[12] S. K. Mazumder, "A novel discrete control strategy for independent stabilization of parallel three-phase boost converters by combining space-vector modulation with variable-structure control," in *Proc. IEEE Trans. Power Electron.*, vol. 18, no. 4, pp. 1070–1083, Jul. 2003.

[13] S. Pettersson and B. Lennartson, "An LMI approach for stability analysis of nonlinear systems," in *Proc. Eur. Control Conf.*, 1997, pp. 1–6.

[14] S. K. Mazumder and K. Acharya, "Multiple Lyapunov function based reaching condition analyses of switching power converters," in *Proc. IEEE Power Electron. Spec. Conf.*, 2006, pp. 2232–2239.

[15] M. Tahir and S. K. Mazumder, "Markov chain model for performance analysis of transmitter power control in wireless MAC protocol: Towards delay minimization in power-network control," in *Proc. IEEE Int. Conf. Adv. Inf. Netw. Appl.*, 2007, pp. 909–916.

Sudip K. Mazumder (SM'02) received the M.S. degree from Rensselaer Polytechnic Institute, Troy, NY, in 1993 and the Ph.D. degree from Virginia Polytechnic Institute and State University, Blacksbury, in 2001.

He is currently the Director of Laboratory for Energy and Switching-Electronics Systems and an Associate Professor in the Department of Electrical and Computer Engineering at the University of Illinois, Chicago. He has over 15 years of professional experience and has held R&D and design positions in leading industrial organizations. His current research interests include interactive power electronics/power networks, renewable and alternative energy systems, photonically triggered and wide-bandgap-based power semiconductor devices, and applied technologies.

Mr. Mazumder is the Chair for the Student/Industry Coordination Activities for the 2009 and 2010 IEEE Energy Conversion Congress and Exposition. He is the Technical Program Committee Cochair for the 2010 IEEE International Symposium on Power Electronics for Distributed Generation Systems. He also serves as the Cochair for the IEEE Power Electronics Society Sustainable Energy Systems Technical Committee. He is an Associate Editor for the IEEE TRANSACTIONS ON INDUSTRIAL ELECTRONICS and the IEEE TRANSACTIONS ON AEROSPACE AND ELECTRONIC SYSTEMS since 2003 and 2008, respectively. He was the Associate Editor for the IEEE POWER ELECTRONICS LETTERS between 2002 and 2005 and was the Editor-in-Chief for the *International Journal of Power Management Electronics* between 2006 and 2009. He received the prestigious 2008 Faculty Research Award and the 2006 Diamond Award from the University of Illinois for outstanding research performance. He also received the Office of Naval Research Young Investigator Award and the National Science Foundation CAREER Award in 2005 and 2002, respectively, and the IEEE TRANSACTIONS ON POWER ELECTRONICS Prize Paper Award in 2002. He also coreceived the 2007 IEEE Outstanding Student Paper Award at the IEEE International Conference on Advanced Information Networking and Applications (with Dr. Muhammad Tahir). He has been invited by the IEEE and the ASME as well as multiple industries, federal agencies, national laboratories, and universities for several keynote, plenary, and invited lectures and presentations.

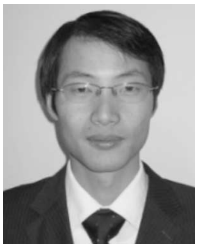

Rongjun Huang (S'05) received the Bachelor of Engineering and Master of Engineering degrees from Jiaotong University, Beijing, China, in 1998 and 2001, respectively, both in electrical engineering, and the Ph.D. degree from the Laboratory for Energy and Switching-Electronics Systems, Department of Electrical and Computer Engineering, University of Illinois, Chicago, in 2009.

In 2001, he was an R&D Engineer with Huawei Technologies, China. Currently, he is with International Rectifier, El Segundo, CA. His research interests include power electronics for renewable energy sources, wide-bandgap power semiconductors, and energy harvesting. He is the author or coauthor of more than ten refereed international journal and conference papers. He serves as a Reviewer for the IEEE TRANSACTIONS ON INDUSTRIAL ELECTRONICS, the IEEE TRANSACTIONS ON AEROSPACE AND ELECTRONIC SYSTEMS, and several international conferences.

Kaustuva Acharya received the Bachelor of Engineering degree in electronics and communication engineering from the Regional Engineering College (now, the National Institute of Technology), Bhopal, India, in 2000, the Master of Science degree in electrical engineering from the University of Illinois, Chicago, in 2003, and the Ph.D. degree in electrical engineering from the University of Illinois, Chicago, in 2008.

Between 2003 and 2008, he was a Research Assistant at the Laboratory for Energy and Switching-Electronics Systems, University of Illinois, Chicago, where subsequently he was a Postdoctoral Research Associate between 2008 and 2009 before accepting a position at Texas Instruments, Dallas. His current research interests include power electronics for renewable and alternate energy sources, and modeling, analyses, and control of interactive power networks for distributed power systems. He is the author or coauthor of more than 20 refereed international journal and conference papers.

Dr. Acharya is a Reviewer for the IEEE TRANSACTIONS ON POWER ELECTRONICS AND INDUSTRIAL ELECTRONICS and several international conferences. He copresented a tutorial titled "Global Stability Methodologies for Switching Power Converters" at the IEEE Power Electronics Specialists Conference, 2007.